Bull Eng Geol Environ (2014) 73:791–799
DOI 10.1007/s10064-014-0583-y

ORIGINAL PAPER

Relationship between static and dynamic elastic modulus of calcarenite heated at different temperatures: the San Julián's stone

V. Brotons · R. Tomás · S. Ivorra · A. Grediaga

Received: 13 July 2013 / Accepted: 18 February 2014 / Published online: 12 March 2014

Abstract The San Julián's stone is the main material used to build the most important historical buildings in Alicante city (Spain). This paper describes the analysis developed to obtain the relationship between the static and the dynamic modulus of this sedimentary rock heated at different temperatures. The rock specimens have been subjected to heating processes at different temperatures to produce different levels of weathering on 24 specimens. The static and dynamic modulus has been measured for every specimen by means of the ISRM standard and ultrasonic tests, respectively. Finally, two analytic formulas are proposed for the relationship between the static and the dynamic modulus for this stone. The results have been compared with some relationships proposed by different researchers for other types of rock. The expressions presented in this paper can be useful for the analysis, using non-destructive techniques, of the integrity level of historical constructions built with San Julián's stone affected by fires.

Keywords Non-destructive techniques · Calcarenite stone · Elastic dynamic modulus · Elastic static modulus · San Julián's stone · Temperature

V. Brotons (✉) · R. Tomás · S. Ivorra
Departamento de Ingeniería Civil, Escuela Politécnica Superior, Universidad de Alicante, P.O. Box 99, 03080 Alicante, Spain
e-mail: vicente.brotons@ua.es

A. Grediaga
Departamento de Tecnología Informática y Computación, Escuela Politécnica Superior, Universidad de Alicante, P.O. Box 99, 03080 Alicante, Spain

Introduction

The Young's modulus, also called elastic modulus, is one of the most important mechanical characteristic parameters of the rocks in relation to use as a construction material. This parameter varies with the degree of weathering of the rock. As a consequence it is essential in engineering to state the value of the modulus corresponding to the different weathering states, taking as a reference the unaltered Young's modulus. Usually, it is not possible to perform static laboratory tests from drilled samples (e.g. in historical buildings) and modulus must be obtained from ultrasonic testing. Because the static modulus (E_{st}) is required for computing the deformations of a building after it comes into service under the applied loads, the static modulus, obtained from conventional laboratory procedures, is required. In these cases in which it is not possible to perform destructive tests to determine the characteristics of the rock, the use of non-destructive techniques using mobile devices constitutes an alternative option.

The dynamically determined elastic modulus (E_{dyn}) is generally higher than that statically determined, and both methods provide high divergent results for low elasticity modulus rocks (Ide 1936). Several studies (e.g. Ide 1936; Vanheerden 1987; Al-Shayea 2004; Kolesnikov 2009) explain these differences by means of the nonlinear elastic response at different ranges of amplitude of the strains ($\in$) involved in the distinct techniques. Other authors (Kolesnikov 2009; Ciccotti and Mulargia 2004) consider that the static test is a dynamic test at a very low frequency, and they highlight the nonlinear elastic response to different associated frequencies (f). Kolesnikov (2009) uses the Kjartansson constant Q-model (Kjartansson 1979) to analyse the effects of intrinsic dispersion of pressure wave velocities in absorbing media (and it is well known that all

rocks absorb energy of elastic waves to a greater or lesser extent). By means of static and dynamic tests, this author obtains the experimental estimation of the possible effect of intrinsic velocity dispersion on the results of the elastic modulus measurements, and concludes that the frequency (f) about 3×10^{-4} Hz corresponds to the observed ratio $E_{st}/E_{dyn} = 0.57$, and must be associated to its static test. Ciccotti and Mulargia (2004) noted that because their tests have a typical duration of about 20 min, the static measurements must be associated with a frequency of approximately 10^{-3} Hz. Both frequency and amplitude of strains are parameters with an important influence on the viscoelastic behaviour of the material (Kjartansson 1979). Ciccotti and Mulargia performed different tests on high-strength limestone samples (i.e. more than 75 MPa), covering a wide range of frequencies and strains. They found no significant dependence of the measured modulus with respect to the two studied variables. The difference between the static and the dynamic modulus is also explained considering the differential effects of porosity, size, and spatial orientation of cracks or bedding planes on both different measurement techniques (Ide 1936; Eissa and Kazi 1988; King 1983; Al-Shayea 2004; Vanheerden 1987). The static method, which is necessary for quantifying the rock deformability, is more sensitive to the presence of discontinuities in the rock. The study of a high-strength limestone (i.e. 70 MPa) (Al-Shayea 2004) showed that the ratio between both moduli:

$$k = E_{dyn}/E_{st} \tag{1}$$

is close to one for static modulus measured at very low loading levels ($\sim$10 % of uniaxial compressive strength). The dynamic modulus (E_{dyn}) and Poisson's ratio (v_{dyn}) are usually computed from Eqs. (2) and (3):

$$E_{dyn} = \rho_{bulk} V_s^2 \frac{\left(4V_s^2 - 3V_p^2\right)}{\left(V_s^2 - V_p^2\right)} \tag{2}$$

$$v_{dyn} = \frac{V_p^2 - 2V_s^2}{2V_p^2 - 2V_s^2} \tag{3}$$

where E_{dyn} is the dynamic Young's modulus, and v_{dyn} is the Poisson's ratio. V_p is the compressional (P) waves velocity; V_s is the shear (S) waves velocity, and ρ_{bulk} is the bulk density of the material.

The relationships between the static and dynamic moduli for different types of rocks and variation ranges proposed by various authors (King 1983; Vanheerden 1987; Eissa and Kazi 1988; Martinez-Martinez et al. 2012) are summarized in Table 1. Note that Eissa and Kazi (1988) performed a statistical analysis using 76 observations from three different sources of information, for which bulk density is known, defining twelve different variables including E_{st}, E_{dyn}, ρ_{bulk}, and nine combinations of them. Each defined variable was correlated with the remaining variables, covering all the possible combinations, and leading to the conclusion that the value of the static modulus of elasticity can be best predicted ($r^2 = 0.92$) from the relationship shown in Eq. (7) (Table 1).

Figure 1 shows the plot of the equations included in Table 1 for their respective validity ranges. The relationship defined by Martinez-Martinez et al. (2012) is not included in the plot because this would require us to assume a function that relates the spatial attenuation with the dynamic modulus. Note that in the Vanheerden's (1987) relationship, the four curves that are shown in Fig. 1 correspond to four different sets of a and b values obtained for the stress-level applied to the tested rock (considered stresses are 10, 20, 30 and 40 MPa). Also notice that in order to represent the nonlinear Eissa and Kazi's (1988) equation we have assumed a correlation between bulk density and dynamic modulus based on published data, which is shown in Fig. 1. All curves are represented in the region of $k > 1$ with dynamic modulus values lower than 130 GPa.

The general trend exhibits a k decrease when dynamic modulus increases, for both linear and non-linear regressions. Therefore, it can be stated that for rocks with a high modulus of elasticity the value of k is closer to one.

The main aim of this work is to propose a new correlation for obtaining the static modulus of the San Julián's stone, a stone widely used for historical building construction in Alicante city, from tests with ultrasound waves. For this purpose, unaltered samples of San Julián's stone have been heated at different temperatures in order to accelerate aging of the stone, and consequently, to induce changes in the deformational properties of the rock (i.e. in the elastic modulus). The comparison between the parameters measured from undisturbed and heated samples has provided a significant relationship between elastic and dynamic modulus, which has been compared with the previously mentioned correlations proposed by other authors. The obtained correlations are very useful in non-destructive techniques for evaluating the integrity level of historical constructions affected by fires using non-destructive techniques.

Materials and samples preparation

Block samples were taken from the Serra Grossa hill, located NE of the urban area of Alicante (SE of Spain). This relief consists of gently dipping (150/20), light yellowish–white, fine to medium-grain size biocalcarenites [according to ISRM (1977)]. This succession, up to 150 m

Table 1 Relationship between static (E_{st}) and dynamic (E_{dyn}) moduli proposed by different authors

References	Relationship	R^2	Samples	E_{dyn} range (GPa)	Rock type
King (1983)	$E_{st} = 1.26\,E_{dyn} - 29.5$ (4)	0.82	174	40–120	Igneous-metamorphic
Vanheerden (1987)	$E_{st} = aE_{dyn}^{b}$ (5)	–	–	20–135	Sandstone-granite
Eissa and Kazi (1988)	$E_{st} = 0.74\,E_{dyn} - 0.82$ (6)	0.70	342	5–130	All types
Eissa and Kazi (1988)	$\log_{10}E_{st} = 0.77\log_{10}(\rho_{bulk}E_{dyn}) + 0.02$ (7)	0.92	76	5–130	All types
Martinez-Martinez et al. (2012)	$E_{st} = \frac{E_{dyn}}{3.8\alpha_s^{-0.68}}$ (8)	–	–	5–50	Limestone-marble

Note that ρ_{bulk} in Eissa and Kazi's (1988) equation is originally expressed in grams per cubic centimetre, although in this work it is expressed in SI units. These equations are plotted in Fig. 1

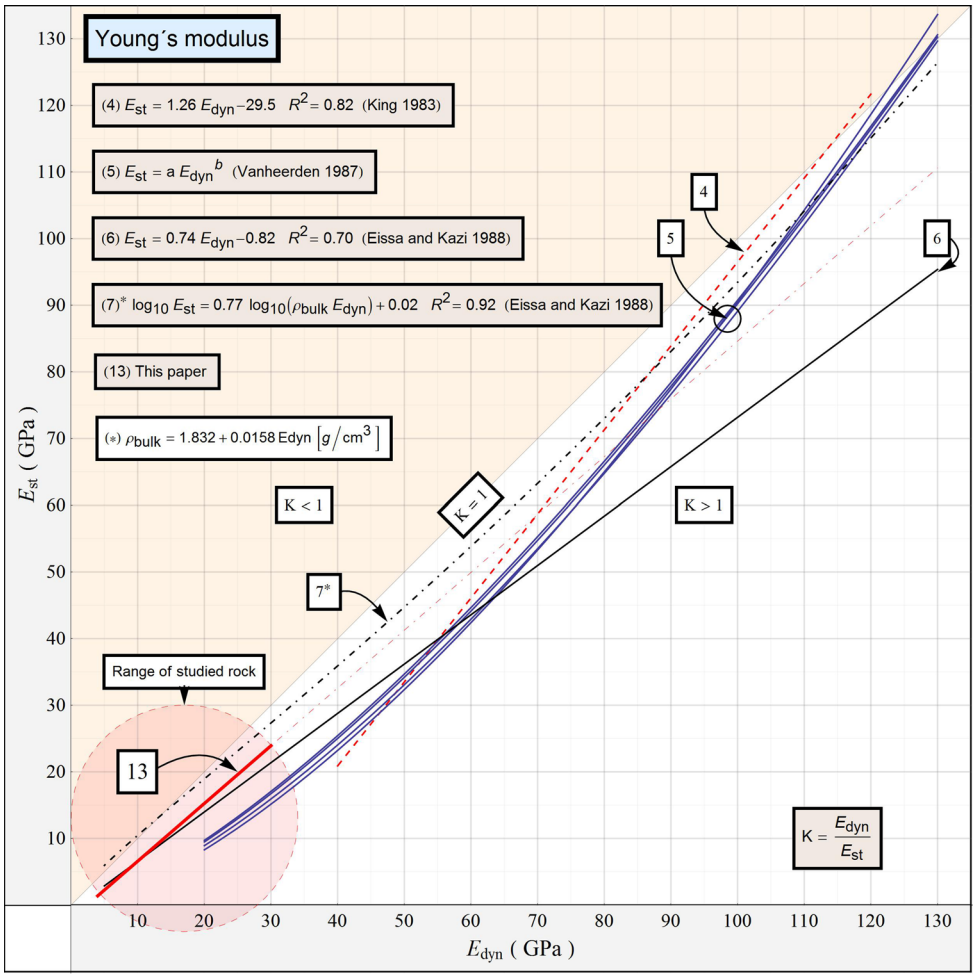

Fig. 1 Plot of the relationship between static and dynamic Young's modulus shown in Table 1. Note that the relationships have been only represented for their range of validity

thick, is upper Miocene in age (Montenat 1977; Montenat et al. 1990).

The rock is locally known as San Julián's stone and has been widely used since the Roman period for the construction of buildings in Alicante city and its surroundings (e.g. Lucentum, the Roman predecessor of the city of Alicante, Santa Bárbara's Castle, City Council building, and Gravina Palace). The specimens studied in this paper were obtained from rock blocks collected from the dump of a railway tunnel under construction. The rock blocks were picked up just after the mechanical excavation and transported to the laboratory, where the samples were extracted by means of a drill. An X-ray diffraction analysis was performed and interpreted using the XPowder software package (Martín 2004). The qualitative search-matching procedure was based on the

Table 2 Summary of physical and mechanical properties of the tested intact rock samples of San Julián's stone

Parameter	Mean	SD	SEM
Bulk density, ρ_{bulk} (KN/m^3)	21.03	0.72	0.15
Open porosity, n_0 (%)	20.8	3.33	0.68
Total porosity, n (%)	22.3	2.72	0.56
Attenuation, α_s (dB/cm)	4.0	0.39	0.08
Young's modulus, *E* (GPa)			
From ultrasonic waves	27.4	3.15	0.64
From mechanical tests[a]	21.6	2.25	1.01
Poisson's ratio, *v*			
From ultrasonic waves	0.24	0.04	0.01
From mechanical tests[a]	0.30	0.08	0.04
Uniaxial compressive strength[a], σ_{ci} (MPa)	31.5	6.01	2.69

[a] The mean values were obtained from 24 samples, except for the mechanical tests that were performed on five rock samples. *SD* standard deviation, *SEM* standard error of the mean

ICDD-PDF2 database. The main components derived from the analysis are: calcite (70 %), iron-rich dolomite (25 %), quartz (5 %), and traces of clay minerals (illite) (Brotons et al. 2013). The studied rock corresponds to a very porous biocalcarenite (a grainstone according to Dunham 1962). From a textural point of view, this rock presents abundant allochemicals, generally smaller than 2 mm size, although bands of various grain sizes have been found. The rock presents a wide variety of fossil bryozoans, foraminifera, red algae, and echinoderm fragments. The orthochemical fraction mainly corresponds to sparite (Louis Cereceda et al. 2001). The studied rock presents medium to high values of open porosity (20.8 ± 3.3 %) and a bulk density of 21.0 ± 0.7 kN/m^3 (according to Spanish standard AENOR 2007). Complementarily, a mercury intrusion porosimetry test has been performed over a representative sample of the studied rock in order to study the pore size distribution. The test indicates that the rock has a macroporosity (>5 μm) of 55.1 % and a microporosity (<5 μm) of 44.9 %, with a mean pore size of 37.52 μm.

For this study, 24 cylindrical samples of 52 mm in diameter and 125 mm long were obtained; the choice of a 2.5 slenderness ratio was made to ensure their suitability for the tests to be conducted according to relevant standards (ISRM 1979). The bases of the cylinders were treated to ensure flatness and perpendicularity relative to the guideline. Table 2 shows the main physical and mechanical properties of the studied rock and the associated errors, where Standard deviation (SD) represents the variance in the values of a variable, whereas the standard error of the mean (SEM) is the standard deviation of the sampling distribution of the mean. Therefore, the SEM provides an idea of the accuracy of the mean, and SD gives an idea of the variability of individual observations. These two parameters are related to each other through the expression:

$$\mathrm{SEM} = \mathrm{SD}/\sqrt{n} \quad (9)$$

where SEM is the standard error of the mean; SD is the standard deviation, and n is the number of samples.

The formula shows that the larger the sample size, the smaller the standard error of the mean. More specifically, the size of the standard error of the mean is inversely proportional to the square root of the sample size.

Note that 24 intact samples were tested for determining the mean values of the different parameters, except for destructive tests (mechanical tests), which were only performed over 5 samples.

The anisotropy of the rock was evaluated by testing six cubic samples of different sizes by means of ultrasonic P-wave velocity (V_p), ultrasonic S-wave velocity (V_s), and spatial attenuation (α_s). The obtained results in three orthogonal directions were highly similar for the tested specimens, providing anisotropy factors (i.e. the ratio between the values measured in two different directions) lower than 1.05 for all the tested samples, indicating a clear isotropic behaviour of the rock.

Table 3 Number of tested samples after heating at different temperatures

Temperature (°C)	Air cooled No. of samples	Water cooled No. of samples	Total
105[a]	5	–	5
200	2	1	3
300	2	1	3
400	3	2	5
500	2	1	3
600	3	2	5
Total	17	7	24

[a] Reference temperature. The 24 samples were previously heated at 105 °C and air cooled for performing non-destructive tests and obtaining reference values. Previous uniaxial compressive strength and mechanical elastic modulus (destructive test) were only obtained for five of these samples in order to determine reference values

Methodology

Heating process

In order to analyse the effect of heating on the rock properties, the specimens were subjected to a heating process at different temperatures. This heating process was performed in an oven in order to reach the target temperature in 60 min. Once target temperatures of 105, 200, 300, 400, 500 and 600 °C were reached for the different samples, the temperatures were kept for 1 h and then cooled in two

different ways (Table 3): air cooled at laboratory temperature and by water immersion at laboratory temperature in a 10 l vessel for 5 min. Finally, the samples were kept dry until the completion of subsequent tests. Table 3 shows the number of tested samples for each condition.

Ultrasonic test

Ultrasonic waves were measured using a signal emitting-receiving device (Panametrics-NDT 5058PR) coupled to an oscilloscope (TDS 3012B-Tektronix), which acquires and digitalizes waveforms, allowing them to be displayed, manipulated, and stored.

Two different kinds of Panametrics transducers were used: a non-polarized transducer couple and an S-polarized transducer couple. The first couple was used in order to acquire the ultrasonic waveform and thereafter to study and quantify the signal in the time domain. The second ultrasonic transducer couple was employed exclusively to measure the S-wave propagation velocity. A visco-elastic couplant was used to achieve good coupling between the transducer and the sample. The frequency of both transducer couples is centred in 1 MHz. Three different ultrasonic parameters were computed from each registered waveform: ultrasonic P-wave velocity (V_p), ultrasonic S-wave velocity (V_s), and spatial attenuation (α_s). P-wave velocity (V_p) is the most widely used ultrasonic parameter, and it was determined from the ratio of the length of the specimen to the transit time of the pulse. The obtained mean values (plus or minus standard deviation) for the 24 tested intact samples were 3.95 ± 0.17 km/s and 2.31 ± 0.12 km/s for the V_p and V_s velocities, respectively, which correspond to a "Medium" velocity range according to Anon (1979).

Spatial attenuation (α_s) quantifies the energy lost during wave propagation through a material. This quantification was performed by comparing the amplitude of the signal emitted (A_e) by the transmitter sensor and the amplitude recorded (A_{mx}) in the signal received by the receptor sensor (Martinez-Martinez et al. 2011). Moreover, spatial attenuation was normalized with respect to the distance between transmitter and receptor sensors (L). α_s (dB/cm) was then calculated according to the next expression:

$$\alpha_s = 20\frac{\log\left(\frac{A_e}{A_{mx}}\right)}{L} \tag{10}$$

The ultrasonic parameters, ultrasonic P-wave velocity (V_p) and ultrasonic S-wave velocity (V_s), have been used to compute the dynamic modulus of the specimens, Young's modulus (E_{dyn}) and Poisson's ratio (v_{dyn}), according to Eqs. (2) and (3).

Uniaxial compressive strength test

For the mechanical tests, an HBM Spider 8 600 Hz device was used jointly with HBM strain gauges (120 Ω, K = 2.1) and Catman v.5.0 analysis software. Longitudinal and transverse strain values were obtained for each loading cycle, up to a maximum value when the applied load is equal to 40 % of the sample ultimate load as specified by the suggested test method (ISRM 1979) for the secant Young's modulus and corresponding Poisson's ratio. A press machine of 200 kN capacity was used for booth compressive strength and elastic properties tests.

Results: relationship between static and dynamic elastic modulus

Figure 2 shows the velocities of P and S waves versus heating temperature for the 24 tested specimens. As it can be seen, there exists a linear trend of both velocities (v_p and v_s) being inversely proportional to temperature (T), with a high coefficient of determination, R^2 [Eqs. (11), (12); Fig. 2]:

$$v_p = 4.291 - 0.004T \tag{11}$$

$$v_s = 2.519 - 0.002T \tag{12}$$

The water-cooled samples show lower propagation velocities for the different temperatures because quick water cooling induces a greater degree of weathering. This weakening and its effect in the wave propagation velocity is typically due to micro-fissuration of calcite crystals.

Note that, although there are two different origins for the dispersion values of E_{dyn} (i.e. the dispersion values of the intrinsic variability from a rock sample to another and the measurement error), only the measurement error of the time of flight for the ultrasonic wave can be computed. In the performed test, the instrumental error is determined by the error in the measurement of the time of flight through the specimen which is up to ±200 ns for the used instruments. Consequently, considering the length and the bulk density of our samples, the error in the estimation of the time leads to an error in the measurement of the velocity which depends on its magnitude. In this case, for the specimen with higher measured velocity values (i.e. with a lower degree of deterioration), it reached 4.114 km/s for the P-wave, and 2.279 m/s for the S-wave; hence the estimation errors for these velocities are ±27 and ±8 m/s. The velocities for the specimen with the lowest measured values (i.e. with a higher degree of deterioration) were 1.491 km/s for the P-wave, and 0.972 m/s for the S-wave, and hence the estimation errors for these velocities are ±4 and ±1 m/s. Thus, considering Eq. (2) these values allow the determination of an error in the computed module

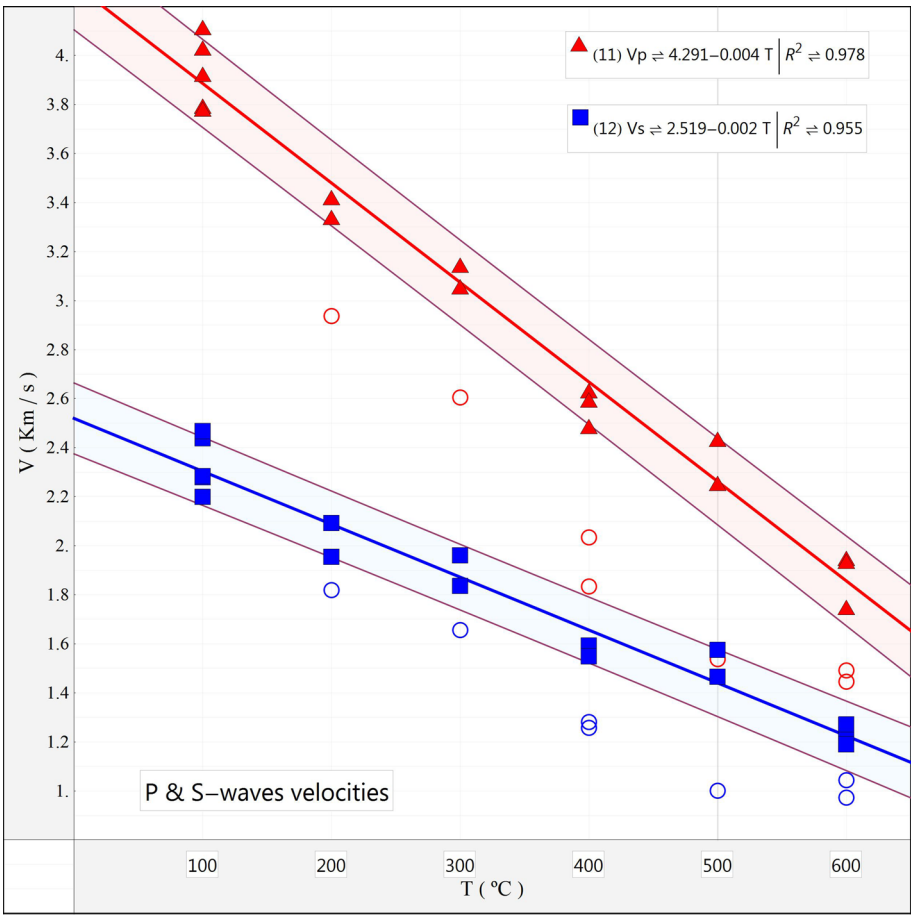

Fig. 2 P (*triangles*) and S (*squares*) wave velocities (V_p and V_s) versus heating temperature (T) of air-cooled samples. Note that *circles* correspond to P and S wave velocities of water-cooled specimens. The decrease of velocity is typically due to micro-fissuration of calcite crystals

which varies between ±0.24 and ±0.02 GPa (with an average value of ±0.11 GPa).

Figure 3 shows the plot of the 24 static and dynamic elastic modules of the different tested samples (blue points) superimposed to the different relationships proposed by the authors cited in the introduction section. As can be seen, all the determined moduli for the San Julián's stone are lower than 50 GPa and are comprised between the two correlations proposed by Eissa and Kazi (1988). k equal to 1 line divides the plotted area, so that the underneath area represents the cases in which the dynamic values are higher than the static. This situation occurs for all samples analysed in this work. We can observe an outlier only in higher values. The obtained elastic modulus and dynamic modulus of each sample have been represented and the best fitting curve has been obtained by means of a least square fitting.

Obtained k-values vary from 1.13 to 2.29. Other authors obtained values between 0.85 and 1.86 (King 1983; Vanheerden 1987; Eissa and Kazi 1988; Al-Shayea 2004) or attributed the differences to natural dispersion of the tested samples and not to the test type (static or dynamic) ($k = 1$) (Ciccotti and Mulargia 2004). Martinez-Martinez et al. (2012) found k-values between 0.5 and 2.1 for carbonate rocks subjected to different aging conditions. This fact implies that the E_{dyn} measured at 1 MHz can range from a half to more than double the mechanical tests measured E_{st}.

In this study the obtained dynamic modulus measured at 1 MHz varied from 30.8 to 4.2 GPa for intact and aged rock samples, respectively, showing a clear dependence of the modulus on aging. The corresponding maximum and minimum static moduli are 24.2 and 2.0 GPa, respectively.

Table 4 shows the correlation coefficient matrix, which shows some significant correlations between the considered parameters. The functions used for the least squares fit are linear in the first five rows and columns (coefficients in bold). In the remaining rows and columns, different functions are used (coefficients in italic).

From Table 4 two strong correlations can be derived. The first one corresponds to the linear correlation between static modulus and dynamic modulus (both in GPa) that provides a coefficient of determination 0.961:

$$E_{st} = 0.867\, E_{dyn} - 2.085 \qquad (13)$$

The second significant correlation provides a decimal logarithm relationship between the static modulus (in GPa), the bulk density (in kg m^{-3}), and the dynamic modulus (in

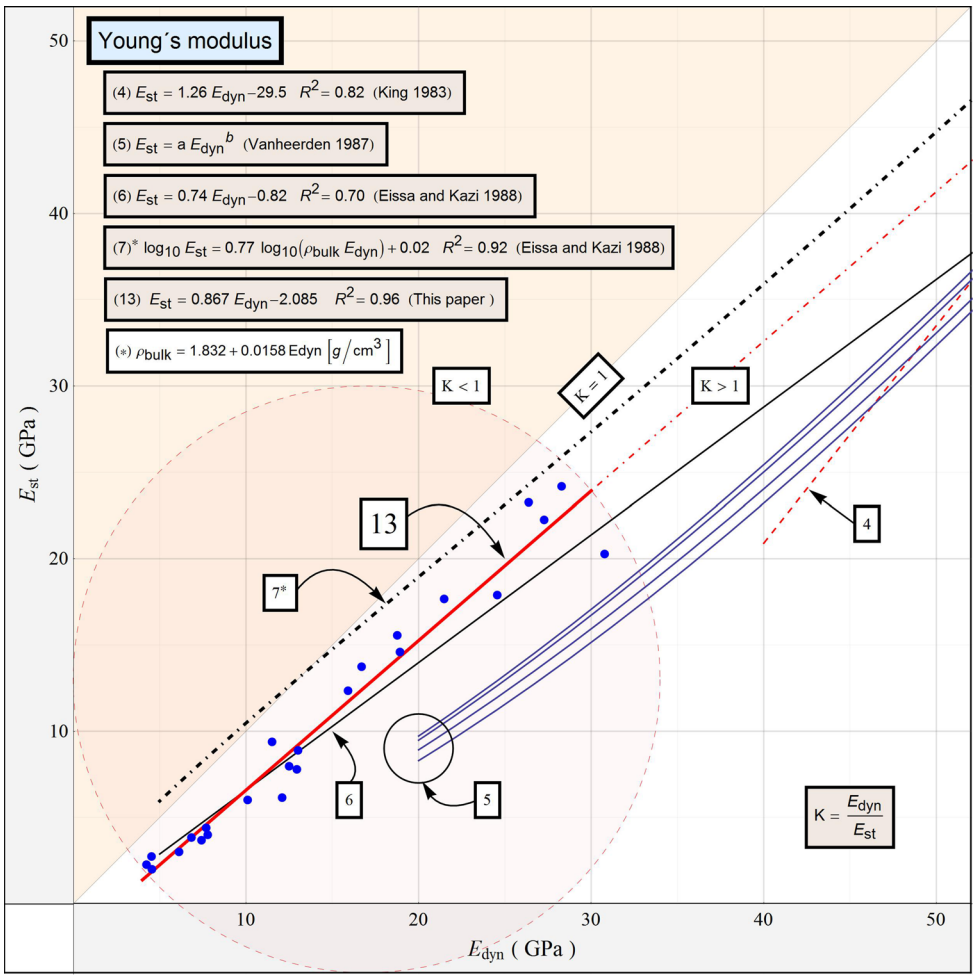

Fig. 3 Representation of the elastic and dynamic Young's modulus relationships proposed by different authors (see Table 1) for low elasticity range (lower than 50 GPa). The relationships have been only represented for their range of validity. *Blue* points correspond to the tested samples

Table 4 Matrix of correlation coefficients

R^2	k	E_{st}	E_{dyn}	α_s	ρ_{bulk}	$m\ \alpha_s^n$	$\log_{10} E_{st}$	$\log_{10}(\rho_{bulk}, E_{dyn})$
k	**1.000**	**0.686**	**0.5687**	**0.272**	**0.074**	*0.268*	–	–
E_{st}		**1.000**	**0.961**	**0.397**	**0.035**	*0.462*	–	–
E_{dyn}			**1.000**	**0.404**	**0.007**	*0.458*	–	–
α_s				**1.000**	**0.001**	–	–	–
ρ_{bulk}					**1.000**	*0.001*	–	–
$m\ \alpha_s^n$						*1.000*	–	–
$\log_{10} E_{st}$							*1.000*	***0.968***
$\log_{10}(\rho_{bulk}, E_{dyn})$								*1.000*

The fitted functions for the first five columns are linear (coefficients in bold). For the remaining columns the fitted functions are non-linear (in italic)

GPa) with a coefficient of determination of 0.968, similar to that proposed by Eissa and Kazi (1988):

$$\log_{10} E_{st} = 1.275 \log_{10}(\rho_{bulk} E_{dyn}) - 4.714 \quad (14)$$

Note that these two correlations have been computed for a calcarenite rock and for low dynamic modulus values (i.e. E_{dyn} from 4 to 30 GPa). Figure 4 shows the plot of the 24 tested samples jointly with the proposed equations [Eqs. (13, 14)]. Regardless of the high value of the coefficient of determination, the residuals randomly dispersed around the horizontal axis indicate that a linear regression model is appropriate for the data. The confidence interval bands of 80 and 95 % are also plotted. The blue dashed line shows the Eq. (14) or nonlinear fit. Since the correlation between density and dynamic modulus found in our tests is very poor, we estimate Eq. (13) is more appropriate than (14) in this case;moreover that the trend of Eq. (14) extrapolated to high dynamic modulus values differs from that shown in Fig. 1.

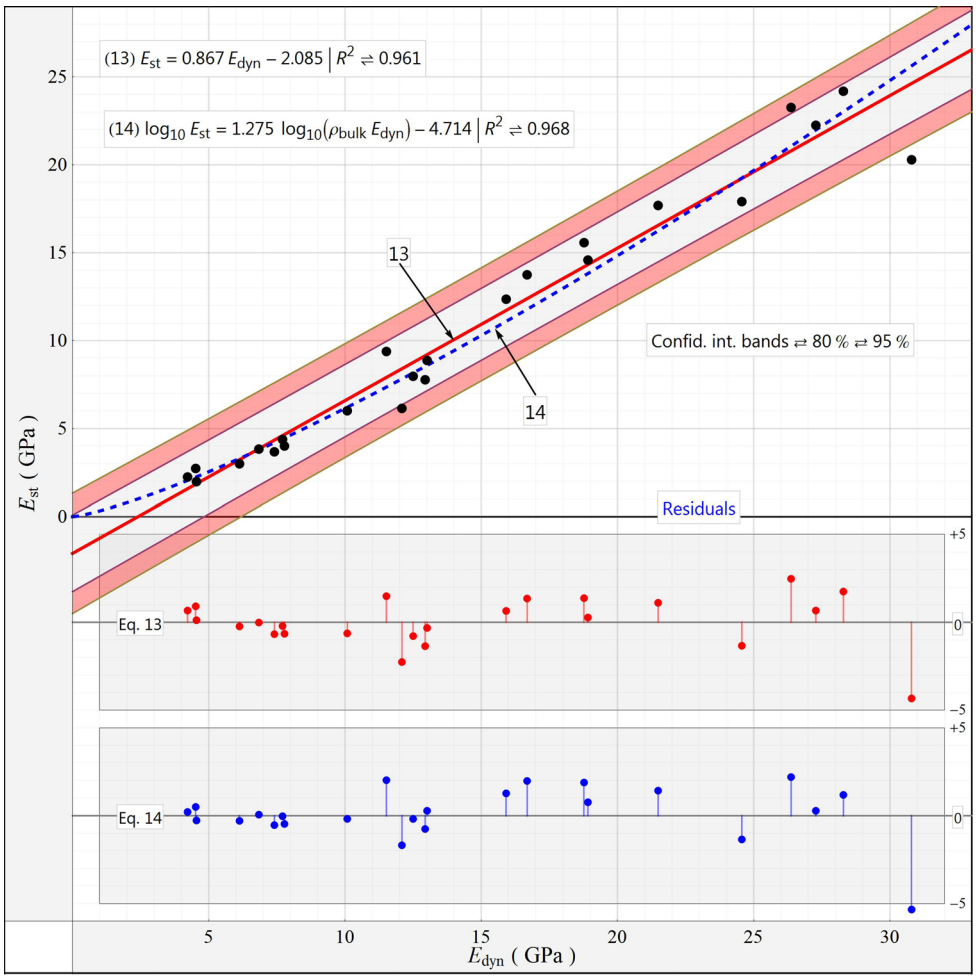

Fig. 4 Linear (Eq. 13) (*red line*) and nonlinear (Eq. 14) (*blue-dashed line*) fitting of the data (*black points*), confidence interval bands (*grey and red shading*), and residuals plot (*blue and red points*)

Conclusion

Generally low elastic modules imply highly fissured or damaged rocks. The mechanical properties, including static modulus, are highly dependent on the size, orientation, and spatial distribution of these cracks. Some studies have shown that P-wave velocity exhibits low sensitivity to these physical characteristics (Martinez-Martinez et al. 2011). This conclusion implies that rocks with different types of cracking, and therefore different values for static and elastic modulus, are, apparently, not different from the viewpoint of the dynamic modulus. This also means that dynamic modulus cannot be used to correct k values. For San Julián's stone it seems to be different. This may be due to the fact that the poor mechanical properties of the studied rock are, essentially, not due to the cracks, but to the weakness of the rock matrix. This same feature makes the fatigue cracks occur in the entire cross section and over the entire body with no preferred orientation, which affects both the mechanical tests and ultrasonic wave propagation. This provides a good correlation between the static modulus and the dynamic modulus. The studied calcarenite behaves differently from metamorphic carbonated rocks. The general trends in the published works for both non-linear and linear adjustments show that the higher the dynamic modulus is, the lower the k values are (Fig. 1). So for very high modulus, k value approaches to one. This is consistent with the fact that very high values of the elastic modulus indicate very compact rocks with a very low porosity, not cracked, and with minimal features able to differentially affect the static and dynamic testing.

The Eqs. (7) and (14) which take into account the bulk density of the material seem to better fit the observations over the entire band of modulus, from low to very high values, but present the disadvantage that, for representing the full band, a correlation between bulk density and dynamic modulus must to be assumed . Moreover, bulk density does not vary continuously over the range (this question will be the aim of further studies). For very high dynamic modulus, the correction that the bulk introduces provides predictions of k near one, which is consistent with other studies (King 1983; Vanheerden 1987; Eissa and

Kazi 1988; Al-Shayea 2004; Ide 1936). For those applications in which it is necessary to study the same type of rock under different weathering degrees, it may be more convenient to use a linear adjustment, as in Eq. (13), for the 4–30 GPa band, ranging from intact rock to very weakened rock. In these cases, bulk density exhibits a low variation, and it is not directly related with the deterioration of mechanical properties. Note that equations similar to (13) also implicitly include the bulk density because the dynamic elastic modulus depends on it [see Eq. (2)]. However, equations similar to (14) are expressed as a function of the square of the bulk density.

Summarizing, it is concluded that static modulus can be obtained from dynamic tests, as shown in Eq. (13) for the studied range (i.e. Edyn values lower than 50 GPa) and for soft rocks. Furthermore, the dynamic modulus (i.e. ultrasonic wave velocity) has been found to be a good indicator of the material degree of deterioration, in this case poorly detected by other parameters such as the attenuation of the ultrasonic wave.

The obtained relationships will allow the computation of the static modulus of elements of cultural heritage of Alicante city made of San Julián's stone (e.g. Gravina Palace, Santa Bárbara Castle, City Council building, Lonja, Principal Theatre, Cathedral of St. Nicholas, Basilica of Santa María) from non-destructive field tests, for the analysis of the integrity level of historical constructions affected by high temperatures. Furthermore, these results can be extrapolated, performing the adequate adaptations, for building stones with similar properties.

Acknowledgments The authors would like to thank Dr. D. Benavente and Dr. J. Martínez from the Earth Sciences Department and Applied Petrology Laboratory from the University of Alicante for allowing us to perform ultrasonic tests on their laboratories and Dr. J. M. Ortega from the Department of Civil Engineering from the University of Alicante for kindly performing the mercury intrusion porosimetry test. The companies U.T.E. FCC Construcción, S.A. and Enrique Ortiz e Hijos Contratistas de Obras, S.A. provided the rock samples from the TRAM tunnel excavation. This work has been partially funded by the University of Alicante projects uausti11–11 and gre09–40, the Spanish National project BIA2012-34316, and the Generalitat Valenciana project gv/2011/044.

References

AENOR (2007) UNE-EN 1936: Métodos de ensayo para piedra natural. Determinación de la densidad real y aparente y de la porosidad abierta y total, vol 1. Asociación Española de Normalización y Certificación (Ed.), Spain. https://www.aenor.es

Al-Shayea NA (2004) Effects of testing methods and conditions on the elastic properties of limestone rock. Eng Geol 74(1–2):139–156. doi:10.1016/j.enggeo.2004.03.007

Anon (1979) Classification of rocks and soils for engineering geological mapping part I: rock and soil materials. Bull Int Assoc Eng Geol 19(1):364–371. doi:10.1007/bf02600503

Brotons V, Ivorra S, Martínez-Martínez J, Tomás R, Benavente D (2013) Study of creep behavior of a calcarenite: San Julián's stone (Alicante). Mater Constr 62(312). doi:10.3989/mc.2013.06412

Ciccotti M, Mulargia E (2004) Differences between static and dynamic elastic moduli of a typical seismogenic rock. Geophys J Int 157(1):474–477. doi:10.1111/j.1365-246X.2004.02213.x

Dunham RJ (1962) Classification of carbonate rocks according to depositional texture. Mem Am Assoc Pet Geol 1:108–121

Eissa EA, Kazi A (1988) Relation between static and dynamic Young's Moduli of rocks. Int J Rock Mech Min Sci 25(6):479–482. doi:10.1016/0148-9062(88)90987-4

Ide JM (1936) Comparison of statically and dynamically determined young's modulus of rocks. Proc Natl Acad Sci USA 22:81–92. doi:10.1073/pnas.22.2.81

ISRM (1977) Suggested method for petrographic description of rocks. ISRM Suggest Methods 15:41–45

ISRM (1979) SM for determining the uniaxial compressive strength and deformability of rock materials. ISRM Suggest Methods 2:137–140

King MS (1983) Static and dynamic elastic properties of rocks from the Canadian shield. Int J Rock Mech Min Sci 20(5):237–241. doi:10.1016/0148-9062(83)90004-9

Kjartansson E (1979) Constant Q-wave propagation and attenuation. J Geophys Res 84(NB9):4737–4748. doi:10.1029/JB084iB09p04737

Kolesnikov YI (2009) Dispersion effect of velocities on the evaluation of material elasticity. J Min Sci 45(4):347–354

Louis Cereceda M, Garcia-del-Cura MA, Spairani Y, de Blas D (2001) The civil palaces in Gravina Street, Alicante: building stones and salt weathering. Mater Constr 51(262):23–37

Martín JD (2004) Using XPowder: a software package for powder X-ray diffraction analysis. Spain, p 105. http://www.xpowder.com. ISBN 84-609-1497-6

Martinez-Martinez J, Benavente D, Garcia-del-Cura MA (2011) Spatial attenuation: the most sensitive ultrasonic parameter for detecting petrographic features and decay processes in carbonate rocks. Eng Geol 119(3–4):84–95. doi:10.1016/j.enggeo.2011.02.002

Martinez-Martinez J, Benavente D, Garcia-del-Cura MA (2012) Comparison of the static and dynamic elastic modulus in carbonate rocks. Bull Eng Geol Environ 71(2):263–268. doi:10.1007/s10064-011-0399-y

Montenat C (1977) Les basins néogènes et quaternaries du Levant d'Alicante à Murcie (Cordillères Bétiques orientales, Espagne). Stratigraphie, paléontologie et evolution dynamique. Doc Lab Geol, Univ Lyon 69, 345 pp

Montenat C, Ott d'Estevou P, Coppier G (1990) Les basins néogènes entre Alicante et Cartagena. Doc Et Trav IGAL 12–13:313–368

Vanheerden WL (1987) General relations between static and dynamic moduli of rocks. Int J Rock Mech Min Sci 24(6):381–385